

Computational Analysis on Bone Adaptation in Resurfacing Hip Arthroplasty with Valgus-Varus Placement



Nor Aiman Nor Izmin, Fatin Hazwani, Mitsugu Todo,
and Abdul Halim Abdullah

Abstract Resurfacing Hip Arthroplasty (RHA) is one of the solutions for young adults with hip osteoarthritis disease (OA). Despite the positive outcomes that were achieved after RHA, the method also has its risks and complications. Early bone failure might occur as consequences from the insertion of improper implant placement. In this study, an inhomogeneous material model of femoral bone was developed from CT-based images and reconstructed to represent resurfacing hip arthroplasty. Different placement of implant was assigned to investigate the effects of the placement to the bone adaptation. Comparison of the Drucker-Prager equivalent stress between the femur bone models with the presence of implant in varus and valgus was analyzed, hence to understand the possibility of bone failures after arthroplasty. A RHA implant was assigned with material properties of cobalt-chromium. The finite element study was simulating the condition of normal walking, with the loading magnitude applied was based on the patient's body weight. The RHA implant placement is found to have a notable influence to the bone conditions especially on the varus $+18^\circ$ placement with stress increment up to 36.31% in the lateral region of the femur, also 31.61 and 19.34% in the medial region of the femur. Thus, the femoral bone models implanted in varus placement shows a higher possibility of bone failures in all conditions.

Keywords Resurfacing hip arthroplasty · Osteoarthritis · Bone failure · Finite element analysis · CT-based image

N. A. N. Izmin · A. H. Abdullah (✉)
Faculty of Mechanical Engineering, Universiti Teknologi MARA (UiTM), 40450 Shah Alam,
Selangor, Malaysia
e-mail: halim471@uitm.edu.my

F. Hazwani
Interdisciplinary Graduate School of Engineering Sciences, Kyushu University, 6-1 Kasuga-Koen,
Kasuga 816-8580, Japan

M. Todo
Research Institute for Applied Mechanics, Kyushu University, 6-1 Kasuga-Koen, Kasuga
816-8580, Japan

1 Introduction

Osteoarthritis (OA) is known as one of the top disabling diseases in the world which can occur at fingers, knees, and hips [1]. In regards to hip, the increment in cases for young adults with hip OA disease should be taken as an important matter nowadays. Despite the thought that hip OA disease only affecting the elderly, however, there are huge numbers of people suffering the hip OA since their young age [2]. The young adults with age under 65 years had to live with pain and disability for decades. A recent study from the Netherlands reported that around 0.44% annual incidence of people is suffering from the groin or hip pain with age between 15 and 60 years old [3]. Meanwhile, in the Asian countries, the hip OA is far less well-known than within the Caucasian population [4]. However, a study published by Takeyama et al. shows that the number of consecutive patients who underwent the primary surgery for hip OA in their institution is quite huge [5]. The patients were all Asian and a total of 978 hips from 843 patients with hip OA were investigated. The average age during the time of surgery was 54.8 years. Thus it is important to extend further information on the solution towards the young patients with hip OA.

Resurfacing hip arthroplasty (RHA) is one of the hip replacement surgeries that replacing the damaged hip joint with a smooth metal surface. This method is suitable for young adults with hip OA, as a way to solve their pain and disability problems [6–9]. Previously, the conventional method Total Hip Arthroplasty (THA) was conducted. However, high failure rates were reported when the THA method is implemented to the young adults [10]. The failure rates were really low after implementing the RHA to the young adults with only 0.02% revision, 1 out of 440 resurfacing hips performed from 384 patients [11]. Besides, the movement and walking pattern of patients who underwent the RHA are also similar to the normal and healthy person for every successful surgery, compared to the patients after THA [12].

Despite the benefits and high survival rates of RHA to young adults, still, the method has its risks and complications. According to Shimmin et al. [13], several complications that usually found after hip surgery (THA and RHA) are vascular damage, thromboembolic disease, nerve palsies, dislocation of the femoral component, heterotopic ossification, aseptic loosening, avascular necrosis, and femoral neck fracture. However, the complication of femoral neck fracture only occurred in RHA since the approach in this method is preserving the neck of the femoral bone [14–17]. Based on the Australian national audit on the first 3429 consecutive patients who underwent the RHA, there were 50 cases of femoral neck fracture have been reported [18]. The mean ages of patients for men and women are 62.05 and 56.17 respectively. Also, the time of the fracture to occur after the surgery was around 15.4 weeks which is considered an early-stage failure. Few factors that might contribute to the risk of femoral bone failure have been discussed previously [18–20]. Nonetheless, one of the important factors that might contribute to bone failure after RHA is the surgical factor. The surgical factor is often associated with the placement of the RHA implant during the surgical procedure. Different placement of the RHA implant might affect

the bone condition and lowering the potential of bone survival, thus leading to the utmost complication which is the failure of the bone.

Therefore, the present study aims to analyze the effects of RHA implant placements towards the femoral bone adaptation of a hip OA patient using finite element (FE) analysis. Several placements of RHA implant were developed in the analysis to predict the stress distribution within the proximal area of the femur, hence understanding the possibility of bone failure after RHA.

2 Development of Inhomogeneous Model from CT-Images

The model of the femoral bone was developed from a computed tomography image of a young adult with hip OA disease. The 47 years old patient is having a hip OA on his left femur with a bodyweight of 87.6 kg. A CT-based image of the patient was acquired in a standard DICOM format, before extracting the CT image by using a biomedical software, Mechanical Finder v10. All the modeling procedures have been conducted by using the software. Previous studies on FE analysis related to biomechanics were using homogeneous types of bone models with several limitations had been stated by the authors [21–24]. Thus, an inhomogeneous femoral bone model has been used in this study as an improvement, also applying the suggestion made by the previous literature. The development of the inhomogeneous bone model was based on the linear relationship between gray scales area and the ‘apparent density’ of the CT image. The solid element of the femoral bone model was generated based on the CT value before proceeds with the calculation of density. The calculation of density was referred to the study made by Keyak et al. [25, 26] to estimate the young’s modulus and bone mineral density (BMD) of the bone (Fig. 1). Table 1 shows the estimation of young’s modulus and yield strength based on the density range of the CT image.

3 Reconstruction of Resurfacing Hip Arthroplasty

In this study, there were 7 placements of RHA implants were developed to the femoral bone model. The placement consists of 3 in varus placement zone, 3 in valgus placement zone, and 1 in straight implant placement. The selected implant placement (varus, straight, and valgus) in this study was based on the previous literature in which the placements have been found in the patients who underwent the RHA.

There were 2 anatomical axes developed on the femoral bone which are the femoral shaft axis and femoral neck axis. The femoral shaft axis is the axis that passing through the center of the femoral bone shaft, while the neck axis is the axis that passes through the center of the femoral bone head. The construction of the straight implant placement of the bone was based on the anatomical axis of the femoral

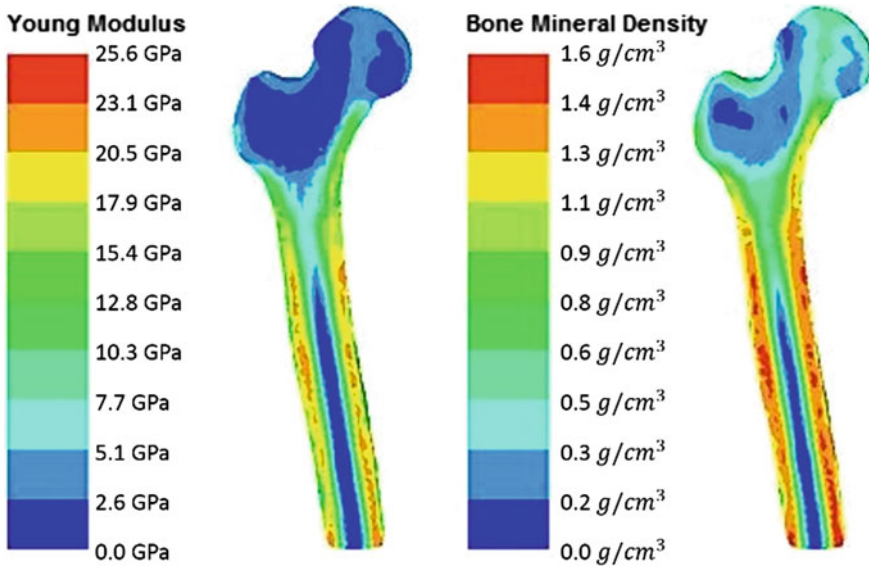


Fig. 1 Variation of young's modulus and bone mineral density (BMD) of the hip OA patient

Table 1 Estimation of young's modulus and yield strength of the inhomogeneous bone model [27]

Density range	Young modulus
$\rho = 0$	$E = 0.001$
$0 < \rho \leq 0.27$	$E = 33900 \rho^{2.20}$
$0.27 < \rho < 0.6$	$E = 5307 \rho + 469$
$0.6 \leq \rho$	$E = 10200 \rho^{2.01}$
$\rho = 0$	$E = 0.001$
Density range	Yield strength (MPa)
$\rho \leq 0.2$	$\sigma_r = 1.0 \times 10^{20}$
$0.2 < \rho < 0.317$	$\sigma_r = 137 \rho^{1.88}$
$0.317 \leq \rho$	$\sigma_r = 114 \rho^{1.72}$

neck. The angle (degree °) between the anatomical neck-shaft axes will become the reference axes in generating the varus and valgus implant placement.

The RHA implant is considered entering the varus placement zone when the implant is inserted into the femoral bone more than the angle of anatomical neck-shaft axes. As for the valgus placement, the implant is considered in the valgus placement zone when it is inserted into the bone less than the angle of anatomical neck-shaft axes [7]. In this study, there were 3 bone models have been developed to each zone (varus and valgus) with increments of 6° orientation between each placement. Thus, the developed placements were between the ranges of 6–18° in each zone. The developed placement of the implant in this study was selected according to the zone

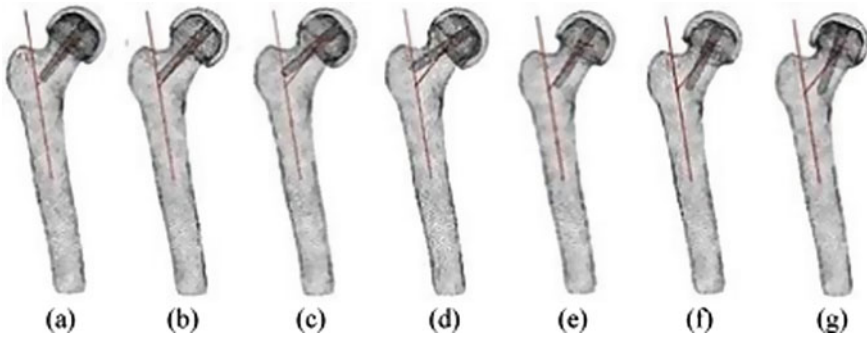


Fig. 2 RHA models with **a** straight placement, **b** 0° **b** $+6^\circ$ varus **c** $+12^\circ$ varus **d** $+18^\circ$ varus **e** -6° valgus **f** -12° valgus and **g** -18° valgus

Table 2 Material properties of Cobalt-Chromium (CoCr) [28]

Model	Young modulus (GPa)	Poisson ratio	Critical stress (GPa)	Yield stress (GPa)	Density (g/cm^3)
Implant	230	0.3	0.94	2.7	8.28

where the implant can be located based on the existing cases reported by the medical institution, where the average values of $6\text{--}18^\circ$ were obtained. Figure 2 shows the example of all models developed in this study with the reference of straight implant placement (Fig. 2a). The type of RHA implant used in this study was the BHR with a femoral head size of 50 mm. The material used for the implant is CoCr with the properties as listed in Table 2.

4 Loading and Boundary Conditions

The loading and boundary conditions applied in this study are simulating the peak load exerted to the femoral bone during the one-leg standing phase of the normal waking condition. According to the experimental study conducted by Bergman et al. [29], about 238% of human body weight will be exerted to the femoral bone head as the hip contact force during normal walking. On another note, Heller et al. [30] suggested that, the most influential muscle that produced the largest force during normal walking is the abductor muscle force, with 104% of the human body weight. Thus, the load magnitude and direction were applied according to both studies, which acted at the femoral bone head for the hip contact force and the greater trochanter of the femoral bone as the abductor muscle force.

5 Effects of Implant Placement to the Femoral Bone Adaptation

The results in this section were discussed by the resulting of Drucker-Prager equivalent stress. Drucker-Prager yield criterion is a failure theory that suitable to the applications with brittle and anisotropic behavior such as bones [27].

5.1 Variation of Drucker-Prager Equivalent Stress

Figure 3 shows the cross-section results of Drucker-Prager equivalent stress between all femur bone models including the intact femur (Fig. 3a). Based on the illustration, the stress shielding phenomena has occurred after the insertion of the RHA implant. The stress reduction can be seen at the femoral head area of the implanted femur as compared to the intact. The phenomenon occurred is believed due to the mismatch of material properties between the bone and the implant. Most of the stress who previously absorbed by the bone is currently taken by the metallic implant after RHA. The stress shielding phenomena might contribute to bone resorption and affecting the strength of the bone which might lead to other bone failures [31].

On another note, the illustration of stress distribution is different between the implanted femur models. Despite the stress reduction that resulting from the stress shielding phenomena, the unnatural increment of stress can be seen between all implanted models. The unnatural increment of stress is believed due to the RHA implant placement. The femoral head area of the femur with valgus placements (Fig. 3c, e) shows lower stress compared to the femur implanted with straight and varus placement (Fig. 3f, h). It is believed that the high concentrated load area at the bone might lead to bone failure when it is exposed to a higher loading impact.

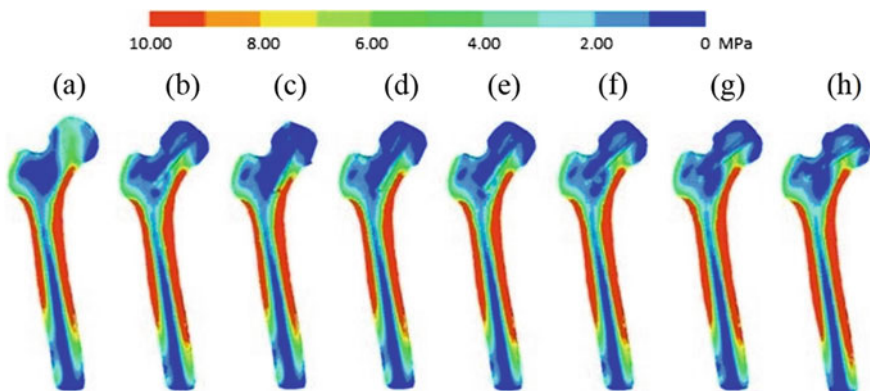


Fig. 3 Drucker-Prager equivalent stress of **a** intact femur **b** straight implant 0° **c** -18° valgus **d** -12° valgus **e** -6° valgus **f** $+6^\circ$ varus **g** $+12^\circ$ varus and **h** $+18^\circ$ varus

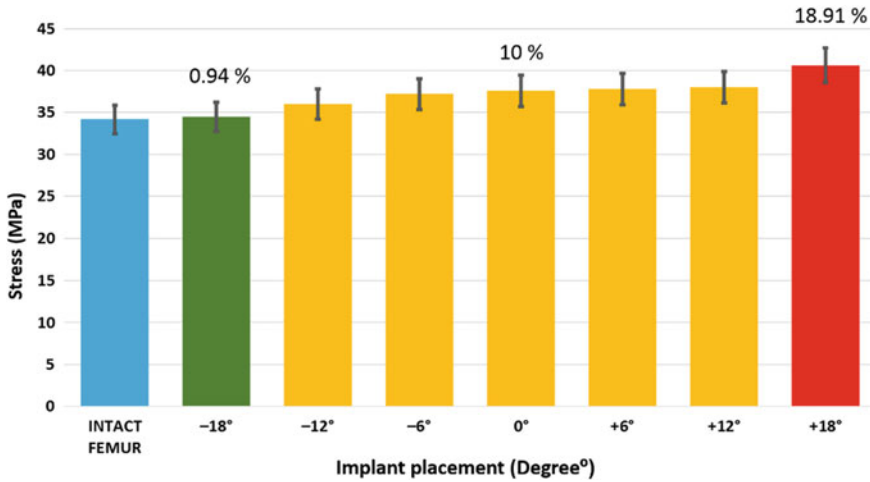


Fig. 4 Comparison of the maximum Drucker-Prager equivalent stress for all models

Therefore, based on the illustration of stress distribution, the implant placement of RHA is affecting the femoral bone condition.

The comparison of the maximum stress value of Drucker-Prager is as shown in Fig. 4. The maximum stress shows an increasing pattern as the implant was oriented from valgus to varus placement zone. The lowest stress value was found at the femur implanted in valgus -18° while the highest stress value was obtained at the femur implanted in varus $+18^\circ$. The comparison between the implanted and the intact femur shows that the stress has increased by 0.94% when the RHA implant was placed to the valgus -18° . As for the straight implant placement, the stress has increased by 10% and for the varus $+18^\circ$, the stress has increased by 18.91%. Thus, it is understood that the implant which has been placed into the varus placement zone might have a higher potential in contributing to early bone failure.

5.2 *Equivalent Stress Distribution Within Medial and Lateral of the Femur*

Three implanted femur models have been selected to compare the stress distribution pattern with the intact femur. It is assumed that the intact femur is having a natural stress distribution as the load was applied since there is no existence of other outsource material. The femur model with valgus -18° , straight implant, and varus $+18^\circ$ has been selected since the significant results were produced by the models. Figure 5 shows the comparison of stress distribution between the intact femur and the selected models. The femur implanted in valgus -18° shows the most similar pattern of stress distribution as compared to the intact femur in both medial and lateral regions. On the

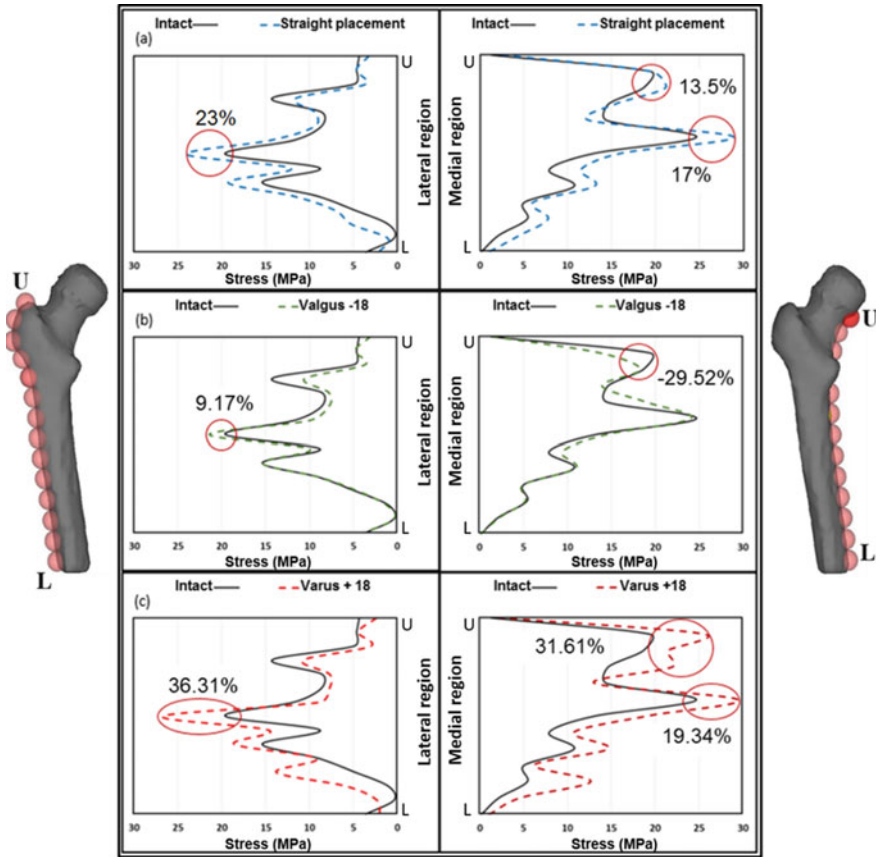


Fig. 5 Stress distribution along U-L within the lateral and medial aspect for **a** intact and straight, **b** intact and valgus -18° and **c** intact and varus $+18^\circ$

lateral aspect, the stress pattern has exceeded the stress produced by the intact with 9.17%, which occurred in the middle region of the femur. As for the medial aspect, stress reduction has produced by the implanted femur with -29.52% as compared to the intact. The straight implant placement (Fig. 5a) also shows an almost similar pattern of stress distribution compared to the intact femur. However, the stress in the lateral aspect of the implanted femur is exceeding the intact by 23% while two increments of stress are found at the medial aspect of the femur. In the proximal area of the medial aspect, the stress of implanted femur has increased by 13.5% and in the middle area, the stress has increased by 17%.

As for the femur model implanted in varus $+18^\circ$ (Fig. 5c), the stress distribution pattern is showing a notable difference as compared to the distribution of the intact femur. At the lateral aspect of the femur, the stress reduction can be seen in the proximal area of the femur, however, the stress has increased by 36.31% at the middle area of the femur. The medial aspect also shows a similar behavior with

a notable difference in stress distribution has produced by the implanted femur. Two increments of stress can be noticed at the proximal and middle areas of the femur with 31.61% and 19.34% respectively which considered as inappropriate stress distribution pattern. Proper stress distribution along the femur bone might enhance the proper development of bone growth. In addition to that, it might also promote long term bone stability [32].

6 Conclusion

The present study shows the importance of RHA implant placement to ensure the femoral bone survival. Different placement of RHA implant demonstrates different outcomes on bone adaptation. Several areas of the femoral bone is having a higher stress concentration as consequences of the implant placement. A femoral bone with an implant inserted in the varus placement might have a higher tendency for bone failure. The finding is found to be similar to the recent study who emphasized the importance of preparing the femoral resurfacing component to the surgeons during the surgical procedure [33] while noted that the varus implant placement should be avoided. On another note, Gamarra et al. mentioned in his study where the valgus placement of the RHA implant appears to have a preventive effect against fracture [34] which also supported the finding in this study.

Acknowledgements This research was supported by Universiti Teknologi MARA, UiTM under Grant No. 600-IRMI/PERDANA 5/3 BESTARI (103/2018). We thank and acknowledge the Ministry of Education, Malaysia, and our colleagues from the Faculty of Medicine, UiTM also Research Institute for Applied Mechanics, Kyushu University, who provided insight and expertise that greatly assisted the research.

References

1. Bijlsma J W J, Berenbaum F, Lefeber F P J G (2011) Osteoarthritis: an update with relevance for clinical practice. *Lancet* 377(9783):2115–2126
2. Drihan J B, Harkey M S, Liu S-H, Salzler M, McAlindon T E (2020) Osteoarthritis and aging: young adults with osteoarthritis. *Curr Epidemiol Rep* 7(1):9–15
3. Röling M A, Mathijssen N M C, Bloem R M (2016) Incidence of symptomatic femoroacetabular impingement in the general population: a prospective registration study. *J Hip Preserv Surg* 3(3):203–207
4. Aimi N, Zamri A, Harith S, Ong Y Q (2019) Prevalence, risk factors and primary prevention of osteoarthritis in asia: a scoping review. *Elderly Health J* 5(1):19–31
5. Takeyama A, Naito M, Shiramizu K, Kiyama T (2009) Prevalence of femoroacetabular impingement in Asian patients with osteoarthritis of the hip. *Int Orthop* 33(5):1229–1232
6. Quesada M J, Marker D R, Mont M A (2008) Metal-on-metal hip resurfacing. *Adv Disadv J Arthroplasty* 23(7):69–73

7. Amanatullah DF, Cheung Y, Di Cesare PE (2010) Hip resurfacing arthroplasty: a review of the evidence for surgical technique, outcome, and complications. *Orthop Clin North Am* 41(2):263–272
8. Isaac GH, Schmalzried TP, Cobb AG, Sullivan TO, Oakeshott RD, Flett M, Vail TP (2006) Development rationale for an articular surface replacement: a science-based evolution. *Proc Inst Mech Eng Part H J Eng Med* 220(2):253–268
9. Wagner P, Olsson H, Ranstam J, Robertsson O, Zheng MH, Lidgren L (2012) Metal-on-metal joint bearings and hematopoietic malignancy: a review. *Acta Orthop* 83(6):553–558
10. Schmalzried TP (2007) Why total hip resurfacing. *J Arthroplasty* 22(7):57–60
11. Daniel J, Pynsent PB, McMinn DJW (2004) Metal-on-metal resurfacing of the hip in patients under the age of 55 years with osteoarthritis. *J Bone Jt Surg Ser B* 86(2):177–184
12. Mont MA, Seyler TM, Ragland PS, Starr R, Erhart J, Bhavsar A (2007) Gait analysis of patients with resurfacing hip arthroplasty compared with hip osteoarthritis and standard total hip arthroplasty. *J Arthroplasty* 22(1):100–108
13. Shimmin AJ, Bare J, Back DL (2005) Complications associated with hip resurfacing arthroplasty. *Orthop Clin North Am* 36(2):187–193
14. Thomas BJ, Amstutz HC (1982) Revision surgery for failed surface arthroplasty of the hip. *Clin Orthop Relat Res* 170:42–49
15. Beaulé PE, Dorey FJ, LeDuff M, Gruen T, Amstutz HC (2004) Risk factors affecting outcome of metal-on-metal surface arthroplasty of the hip. *Clin Orthop Relat Res* 418:87–93
16. Martini F, Leberer C, Mayer F, Leichtle U, Kremling E, Sell S (2000) Precision of the measurements of periprosthetic bone mineral density in hips with a custom-made femoral stem. *J Bone Jt Surg Ser B* 82(7):1065–1071
17. Kishida Y, Sugano N, Nishii T, Miki H, Yamaguchi K, Yoshikawa H (2004) Preservation of the bone mineral density of the femur after surface replacement of the hip. *J Bone Jt Surg Ser B* 86(2):185–189
18. Shimmin AJ (2005) Femoral neck fractures following Birmingham hip resurfacing: a national review of 50 cases. *J Bone Jt Surg Br* 87-B(4):463–464
19. Freeman MA (1978) Some anatomical and mechanical considerations relevant to the surface replacement of the femoral head. *Clin Orthop Relat Res* 134:19–24
20. Freeman MA, Cameron HU, Grown GC (1978) Cemented double cup arthroplasty of the hip: a 5 year experience with the ICLH prosthesis. *Clin Orthop* 134:45–52
21. Radcliffe IAJ, Taylor M (2007) Investigation into the effect of varus-valgus orientation on load transfer in the resurfaced femoral head: a multi-femur finite element analysis. *Clin Biomech* 22(7):780–786
22. Davis ET, Olsen M, Zdero R, Papini M, Waddell JP, Schemitsch EH (2009) A biomechanical and finite element analysis of femoral neck notching during hip resurfacing. *J Biomech Eng* 131(4):041002
23. Murray ET, Polga JJOK, Gill HS, Viceconti M (2012) Strain distribution within the human femur due to physiological and simplified loading: finite element analysis using the muscle standardized femur model. *J Eng Med* 217:173–189
24. Taddei F, Cristofolini L, Martelli S, Gill HS, Viceconti M (2006) Subject-specific finite element models of long bones: an in vitro evaluation of the overall accuracy. *J Biomech* 39(13):2457–2467
25. Keyak JH, Rossi SA, Jones KA, Skinner HB (1997) Prediction of femoral fracture load using automated finite element modeling. *J Biomech* 31(2):125–133
26. Keyak JH, Skinner HB, Fleming JA (2001) Effect of force direction on femoral fracture load for two types of loading conditions. *J Orthop Res* 19(4):539–544
27. Tawara D, Sakamoto J, Murakami H, Kawahara N, Oda J, Tomita K (2010) Mechanical therapeutic effects in osteoporotic L1-vertebrae evaluated by nonlinear patient-specific finite element analysis. *J Biomech Sci Eng* 5(5):499–514
28. Abdullah AH, Todo M, Nakashima Y (2017) Prediction of damage formation in hip arthroplasties by finite element analysis using computed tomography images. *Med Eng Phys* 44:8–15

29. Bergmann G, Deuretzbacher G, Heller MO, Graichen F, Rohlmann A, Strauss J, Duda GN (2001) Hip contact forces and gait patterns from routine activities. *J Biomech* 34(7):859–871
30. Heller MO, Bergmann G, Kassi JP, Claes L, Haas NP, Duda GN (2005) Determination of muscle loading at the hip joint for use in pre-clinical testing. *J Biomech* 38(5):1155–1163
31. Watanabe Y, Shiba N, Matsuo S, Higuchi F, Tagawa Y, Inoue A (2000) Biomechanical study of the resurfacing hip arthroplasty: finite element analysis of the femoral component. *J Arthroplasty* 15(4):505–511
32. Abdullah AH, Jaafar EF, Nasir N, Abdul Latip EN, Tardan G (2011) Influences of prosthesis stem lengths in cementless total hip arthroplasty. *Appl Mech Mater* 52–54:2088–2093
33. Sershon R, Balkissoon R, Valle CJD (2016) Current indications for hip resurfacing arthroplasty in 2016. *Curr Rev Musculoskeletal Med* 9(1):84–92
34. Fraile Gamarra I, Jiménez Viseu Pinheiro JF, Cano Gala C, Blanco Blanco JF (2019) Birmingham mid-head resection periprosthetic fractures: case report. *Int J Surg Case Rep* 64:174–176